B-T-3255

The Diffusion Bonding of Silicon Carbide and Boron Carbide Using Refractory Metals

B.V. Cockeram

USDOE Contract No. DE-AC11-98PN38206

BETTIS ATOMIC POWER LABORATORY WEST MIFFLIN, PENNSYLVANIA 15122-0079

Operated for the U.S. Department of Energy
by Bechtel Bettis, Inc.

DISCLAIMER

Portions of this document may be illegible in electronic image products. Images are produced from the best available original document.

The Diffusion Bonding of Silicon Carbide and Boron Carbide Using Refractory Metals

B.V. Cockeram, Bettis Atomic Power Laboratory, P.O. Box 79, West Mifflin, PA 15122-0079.

Abstract

Joining is an enabling technology for the application of structural ceramics at high temperatures. Metal foil diffusion bonding is a simple process for joining silicon carbide or boron carbide by solid-state, diffusive conversion of the metal foil into carbide and silicide compounds that produce bonding. Metal diffusion bonding trials were performed using thin foils (5 μm to 100 μm) of refractory metals (niobium, titanium, tungsten, and molybdenum) with plates of silicon carbide (both α-SiC and β-SiC) or boron carbide that were lapped flat prior to bonding. The influence of bonding temperature, bonding pressure, and foil thickness on bond quality was determined from metallographic inspection of the bonds. The microstructure and phases in the joint region of the diffusion bonds were evaluated using SEM, microprobe, and AES analysis. The use of molybdenum foil appeared to result in the highest quality bond of the metal foils evaluated for the diffusion bonding of silicon carbide and boron carbide. Bonding pressure appeared to have little influence on bond quality. The use of a thinner metal foil improved the bond quality. The microstructure of the bond region produced with either the α-SiC and β-SiC polytypes were similar.

Introduction

The bonding of ceramics such as silicon carbide (SiC) and boron carbide (B_4C) is an enabling technology for the broader engineering application of these materials. Although many different approaches have been taken to join SiC or B_4C, the use of polymer precursors, glass bonding, melt infiltration, and metal diffusion bonding are methods that can be performed at practical processing temperatures. Any of these methods can be used to produce joints with high-temperature strength.

Metal diffusion bonding results from solid-state, diffusive conversion of a metal insert into silicide, boride, and/or carbide compounds that produce strong joints. Metal diffusion bonding of SiC has been achieved with refractory metals such as titanium, molybdenum, tantalum, and niobium [1-8]. Most of previous diffusion bonding studies have involved the use of sintered or hot-pressed SiC, which has the hexagonal α-SiC structure [9]. One goal of this work is to evaluate titanium, molybdenum, niobium, and tungsten diffusion bonding of Chemical Vapor Deposited (CVD) SiC, which has a cubic β-SiC structure [9]. To our knowledge the use of tungsten foil for diffusion bonding has not been previously evaluated.

Little work has been done on the diffusion bonding of B_4C with metal foils. Some information on diffusion between B_4C and bulk titanium or bulk molybdenum has been reported [8,10]. The purpose of this work is to preliminarily evaluate the viability of using a metal foil diffusion bonding processes to produce joints for β-SiC or B_4C. The microstructural characterization of the bond regions is reported.

Metal Diffusion Bonding

Refractory metal carbides such as NbC, TiC, Mo_2C, and WC are thermodynamically more stable than SiC [11]. Intimate contact between a refractory metal foil and SiC results in the conversion of the metal (M) into carbide (MC_X) and silicide compounds (MSi_Y) if the metal carbides or silicides are more thermodynamically stable than SiC:

$$(X*Y)SiC + (X+Y)M \rightarrow (Y)MC_X + (X)MSi_Y \qquad (1)$$

Metal diffusion bonding is produced by the solid-state, diffusive conversion of the metal foil insert into carbide and silicide compounds. The kinetics for solid-state diffusion are generally fast enough at temperatures greater than 1200°C to result in full conversion of a thin metal foil insert into the more stable metal-carbide and metal-silicide phases. The quality of the metal foil diffusion bond is generally influenced by the volume change resulting from diffusive conversion of the metal foil into carbide or silicide phases and differences in physical properties between the base ceramic (SiC or B_4C) and the metal-carbide and metal-silicide phases that are formed in the bond region. Thus, metallographic examination and analysis of the phases in the bond region is one approach to preliminarily evaluate the use of specific metal foils for diffusion bonding.

Experimental Procedure

Bonding samples (1.3 cm X 1.3-0.64 cm X 0.32 cm) of Hexoloy™ SA SiC (Carborundum Co, Niagra Falls, NY) and CVD SiC (Morton Advanced Materials, Woburn, MA) were lapped flat to a smooth polish. Hexoloy™ SA SiC is a single-phase, sintered α-SiC product that is 98% theoretical density and contains approximately 0.4% boron as a sintering aid. Morton CVD SiC is single phase β-SiC with 100% theoretical density and 99.99% purity. Bonding samples (1.19 cm X 0.64 cm X 0.32 cm) of $^{11}B_4C$, which were >99% pure with the following impurities: Si = 223.8 ppm, Fe = 708.8 ppm, Mg = 9.4 ppm, Ca = 13.1 ppm, Cr = 36.5 ppm, Al = 14.4 ppm, Ti < 1 ppm, Ni < 1 ppm, and Zr < 1 ppm (Eagle-Picher Industries, Quapaw, OK), were lapped flat and smooth. The $^{11}B_4C$ was 99.46 atomic% enriched in the ^{11}B isotope with a B:C ratio of 4.20±0.20. The free carbon content of the $^{11}B_4C$ was 0.0134 weight% and no soluble boron was detected. Prior to joining, the SiC or $^{11}B_4C$ pieces were cleaned by rinsing with acetone, ultrasonic cleaning in alcohol, rinsing in de-ionized (DI) water, etching for 2-3 minutes in 50% HF acid, and then rinsing in DI water, acetone, and ethanol.

Pure metal foils were used for diffusion bonding (Alfa-Aesar): (1) niobium, 12.7 μm thick, 99.9% pure, (2) molybdenum, 12.7 μm and 25.4 μm thick, 99.9% pure, (3) titanium, 5.1 μm and 25.4 μm thick, 99.9% pure, and (4) tungsten, 50.8 μm thick, 99.95% pure. The tungsten foil was electrolytically thinned in a sodium-hydroxide solution to a thickness of 25 μm. The foils were cleaned in acetone and ethanol prior to joining.

The joining of SiC/metal/SiC or $^{11}B_4C$/metal/$^{11}B_4C$ sandwiches was accomplished using refractory metal clevis fixturing (Ta-10W and TZM grips) in either a vacuum furnace (~10^{-6} torr) or an inert atmosphere (flowing high purity helium) furnace. The majority of the bonding runs were completed in the inert atmosphere furnace that consists of graphite heating elements and graphite insulation. Tantalum foil was wrapped around the fixturing to minimize carbon contamination of the specimens. A dead weight load was applied from the start of the run to produce a compressive pressure of 3.4 to 18.6 MPa with the refractory metal clevis fixturing. The inert atmosphere furnace was pumped down to 10^{-3} torr and then back-filled with helium prior to starting the run. The specimens were heated at a rate of 500 C°/hour to 300C°/hour to a temperature of 1200°C to 1500°C, held for 10 hours, and then furnace cooled.

The bond regions were cross-sectioned, metallographically prepared, and examined using optical microscopy, Electron Microprobe (EMP) and Scanning Electron Microscopy (SEM) with Secondary Electron (SE), Backscattered Electron (BSE), energy dispersive X-ray spectrometry (EDS), and wavelength dispersive X-ray (WDS) capability. Scanning Auger Multiprobe (SAM) analysis was performed on the polished cross-sections to separate peak over-lap between the silicon and metal peaks, and provide a better analysis of light elements (carbon + boron). Due to the beam interaction in the substrate, the analytical volume for EMP or SEM analysis is typically about 2-3 μm in width and 2-3 μm in depth. Since auger electrons are only produced at the surface, the analytical volume for SAM analysis is typically less than 0.1 μm in diameter and 0.01 μm in depth. Thus, SAM analysis provides a finer resolution of the phases in the reaction zones.

Results and Discussion

A. SiC/Nb/SiC Bonds

The bonding of CVD SiC with niobium foil was achieved at 1200°C and 1500°C with 3.4 MPa pressure, but the bond produced at 1500°C appeared to be stronger (Table 1). Metallographic inspection shows that the bond region in Figure 1 contained varying degrees of cracking in bond phases, grain pullout, and delamination between the bond region and the SiC base material, which indicates that the quality of the bond was not ideal. The use of a higher bonding pressure (17.2 MPa) provided no significant improvement in bond quality. Some of these defects could be artifacts from metallographic preparation, but the high density of defects indicates that the quality of the SiC/niobium-foil/SiC joints is relatively poor in comparison to diffusion bonds produced with other metals.

The EMP analysis of the SiC/niobium-foil/SiC joint in Figure 1 indicates that the bond region consists of the following structure: (1) Nb-carbide layer (NbC) at the SiC/bond zone interface, (2) layer of Nb-carbide (NbC) in the exact middle of the bond zone, and (3) multi-phase layer of Nb-silicide phases (mostly $NbSi_2$ with some Nb_5Si_3 and Nb_5Si_3C) and Nb-carbide fingers (likely NbC). Although beam-overlap and errors in the quantification of carbon are large, the relative values provide the basis for the phase identification in Figure 1. The phases identified in the bond region in Figure 1 are the same as the reaction zone phases previously reported for SiC/niobium-foil/SiC bonds formed under similar temperature/time parameters [1,2]. Previous SiC/niobium-foil/SiC bonds [1,2] were produced with hot-pressed or sintered SiC, which has a hexagonal α-SiC type structure. The use of CVD SiC in this work, which has the cubic β-SiC structure, resulted in a similar microstructure in the bond region.

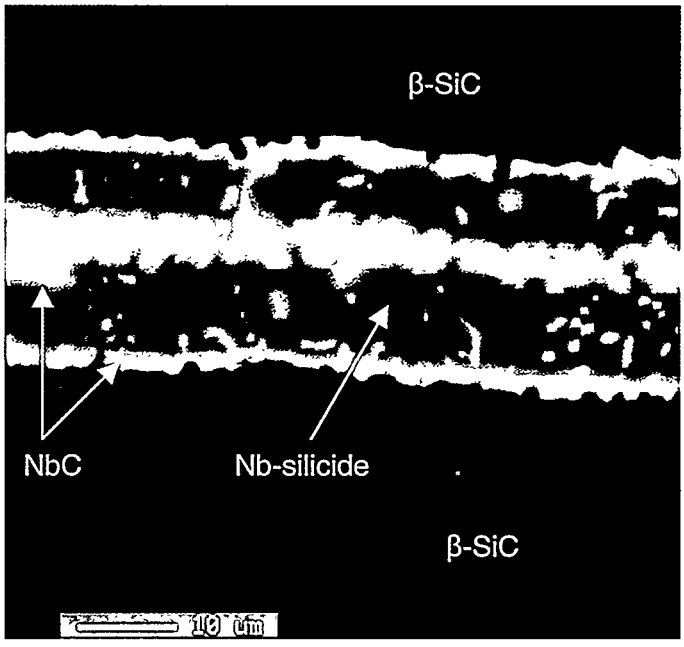

Figure 1. SEM micrograph of the joint region of a SiC/niobium-foil/SiC bond (Run #2 in Table 1).

Based on the bond zone thickness measured in Figure 1 (-25-30 μm) the volume change resulting from diffusive conversion of the 12.5 μm thick niobium foil into the carbide and silicide phases in the bond joint is fairly large (30μm/12.5μm = 2.4), which may produce large growth

Table 1. Summary of coupon types and sizes, foil types, bonding parameters, and general results for the diffusion bonding for SiC/metal-foil/SiC and $^{11}B_4C$/metal-foil/$^{11}B_4C$ sandwiches.

Run #	Foil Type (Thickness in [μm])	Coupons		Bond Run Parameters			Results	Ratio of Final Thickness of Bond Region to initial foil thickness
		Type	Coupon Size [cm]	Temp. [°C]	Time [hours]	Applied Pressure [MPa]		
1	Nb (12.7 μm)	CVD SiC	0.89 X 0.89 X 0.25	1200	10	3.4	Bonding. Poor Quality.	---
2	Nb (12.7 μm)	CVD SiC	0.89 X 0.89 X 0.25	1500	10	3.4	Bonding. Poor Quality.	2.4
3	Nb (12.7 μm)	CVD SiC	0.89 X 0.89 X 0.25	1500	10	17.2	Bonding. Poor Quality.	---
4	Ti (25.4 μm)	CVD SiC	0.89 X 0.89 X 0.25	1500	10	3.4	Bonding. Poor Quality.	1.4
5	Ti (25.4 μm)	CVD SiC	0.89 X 0.89 X 0.25	1400	10	13.8	Bonding. Poor Quality.	---
6	Ti (5.1 μm)	H-SA SiC	1.27 X 1.27 X 0.32	1500	10	8.8	Bonding. Fair Quality.	1.35
7	Mo (12.7 μm)	CVD SiC	0.89 X 0.89 X 0.25	1200	10	3.4	No Bonding.	---
8	Mo (12.7 μm)	CVD SiC	0.89 X 0.89 X 0.25	1500	10	3.4	Bonding. Good Quality.	1.6
9	Mo (12.7 μm)	H-SA SiC	1.27 X 1.27 X 0.32	1500	10	8.8	Bonding. Good Quality.	---
10	Mo (12.7 μm)	H-SA SiC	1.27 X 0.64 X 0.32	1500	10	17.2	Bonding. Good Quality.	---
11	Mo (12.7 μm)	CVD SiC	1.27 X 1.27 X 0.36	1500	10	8.8	Bonding. Good Quality.	---
12	Mo (12.7 μm)	CVD SiC	1.27 X 1.27 X 0.36	1500	10	8.8	Bonding. Good Quality.	---
13	Mo (25.4 μm)	CVD SiC	1.27 X 0.64 X 0.36	1500	10	17.2	Bonding. Fair Quality.	---
14	W (25.4 μm)	H-SA SiC	1.27 X 0.64 X 0.32	1500	10	17.2	Bonding. Fair Quality.	1.4
15	Ti (5.1 μm)	$^{11}B_4C$	1.19 X 0.64 X 0.32	1500	10	18.6	Bonding. Fair Quality.	1.67
16	Mo (12.7 μm)	$^{11}B_4C$	1.19 X 0.64 X 0.32	1500	10	18.6	Bonding. Good Quality.	2.15

H-SA = Hexoloy™ SA SiC (Carborundum Co, Niagra Falls, NY).
CVD = CVD SiC (SiC (Morton Advanced Materials, Woburn, MA).

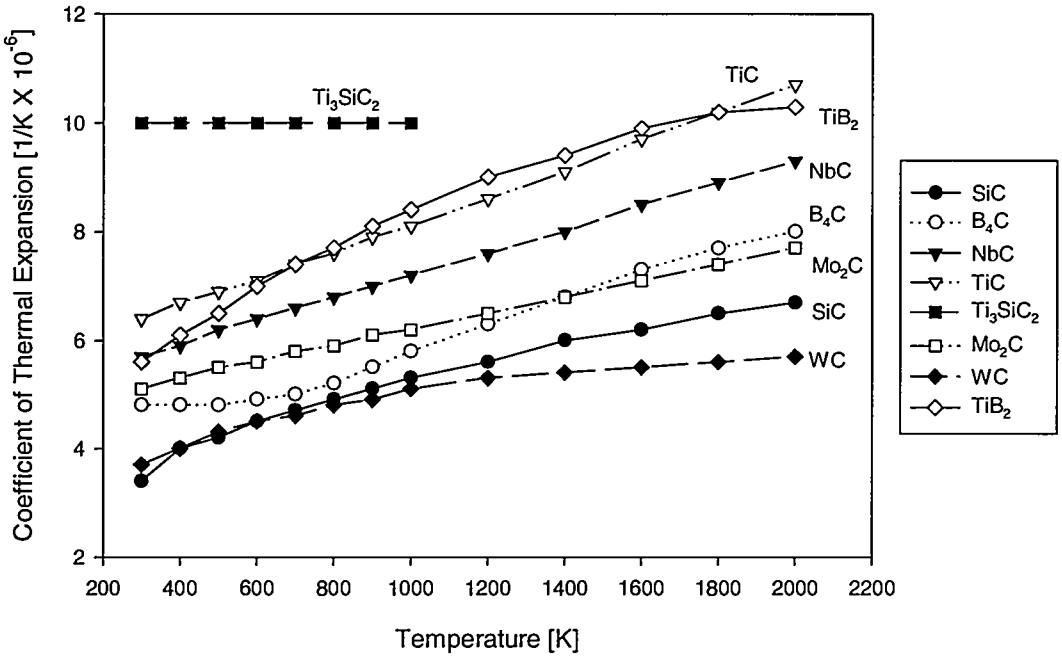

Figure 2. Plot of CTE versus temperature for various carbides and TiB_2 from reference data [12,13].

stresses that result in excessive cracking in the bond joint. Large differences in coefficient of thermal expansion (CTE) between niobium-carbide and SiC also contribute to stresses during heating and cooling, see Figure 2. The brittle niobium-carbide and niobium-silicide phases in the SiC/niobium-foil/SiC joint are apparently susceptible to cracking from these stresses, which results in the formation of defects such as cracks, grain pullout, and bond delamination.

B. SiC/Ti/SiC Bonds

CVD SiC was bonded with 25 μm thick titanium foil using the conditions given in Table 1. Metallographic inspection in Figure 3a indicates that the bond region contained a high density of defects. Many of the bond defects observed metallographically could be preparation artifacts, but the high density of defects indicates that the quality of the SiC/titanium-foil/SiC joints is less desirable in comparison to diffusion bonds produced with other metals. An increase in bonding pressure from 3.4 MPa to 13.8 MPa resulted in little observable improvement in bond quality, see Table 1. The use of a thinner titanium foil (5.1 μm) results in a lower density of defects and higher bond quality, see the metallographic section show in Figure 3b. Thus, the use of a thinner titanium foil insert appears to be a viable approach to improve bond quality.

The EMP analysis of the SiC/Ti/SiC joint in Figure 3a indicates that the bond region consists of a continuous matrix of a needle-like phase containing titanium, silicon, and carbon (Ti_3SiC_2) that surrounds discrete titanium-silicide phases (likely $TiSi_2$, Ti_5Si_3, or $Ti_5Si_3(C)$). Errors in quantifying carbon using EDS/WDS and possible beam interference between phases makes accurate phase identification difficult. The use of Hexaloy™ SiC (α-SiC) with the thinner titanium foil (5.1 μm) resulted in a bond region consisting of a Ti_3SiC_2 matrix with very fine precipitates that are presumably a titanium-silicide phase, see Figure 3b. The use of the thinner foil results in a refinement of the microstructure in the bond region. Titanium diffusion bonding of hot pressed or sintered SiC with the α-SiC structure previously resulted in a bond region microstructure consisting of a Ti_3SiC_2 matrix with titanium-silicide precipitates [3,4,5]. Thus, the bond region microstructure resulting from titanium diffusion bonding of CVD SiC (β-SiC) in this work was similar to that produced with an α-SiC base material. Solid-state diffusive conversion of titanium foil into titanium-silicide and Ti_3SiC_2 phases by reaction with SiC results in a relatively small increase in the joint thickness in Figure 3 (35μm/25μm = 1.4 and 6.9μm/5.1μm = 1.35, see Table 1) with associated growth stresses. Large differences in CTE between Ti_3SiC_2 and SiC shown in Figure 2 likely produce large stresses in the brittle titanium-silicide and Ti_3SiC_2 phases in the bond joint and cause the excessive cracking, pullout, and delamination defects. The use of the thinner titanium foil (5.1 μm) reduces the volume of material with the high CTE mismatch in the bond region, which likely decreases the density of defects.

C. SiC/Mo/SiC Bonds

No bonding was produced at 1200°C with 12.5 μm thick molybdenum foil, but strong bonding was produced at 1500°C with 3.4 MPa of applied pressure, see Table 1. Higher temperatures were needed to achieve strong bonding for either CVD SiC or Hexaloy™ SA SiC with molybdenum foil. A low density of cracks was observed in the bond region of the molybdenum diffusion bond in Figure 4. Any cracks observed in the bond region of the SiC/molybdenum-foil/SiC joints may be artifacts produced by metallographic preparation, but the low density of cracks indicates that the quality of the SiC/molybdenum-foil/SiC bond is significantly better than the diffusion bonds produced with niobium and titanium. The use of higher bonding pressures

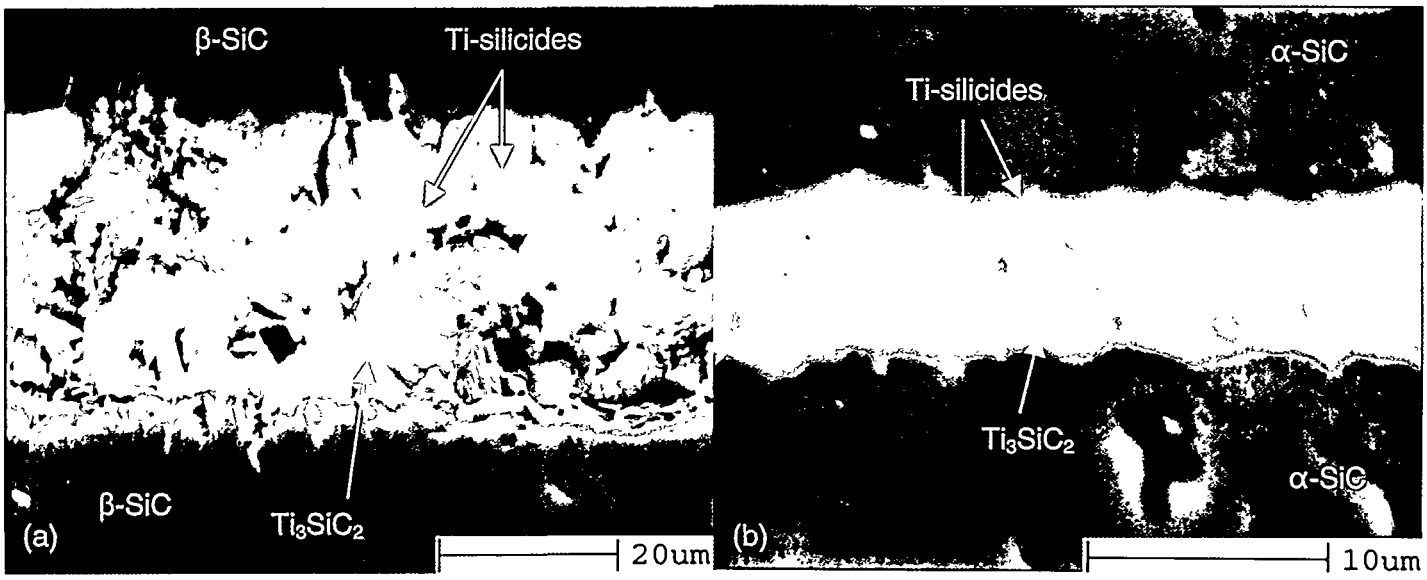

Figure 3. Micrographs of the bond region microstructure of SiC/titanium-foil/SiC diffusion bonds produced under the conditions given in Table 1: (a) Run #4 in Table 1, which involves CVD SiC material with 25 μm thick foil, and (b) Run #6 in Table 1, which involves α-SiC with 5.1 μm thick foil.

(8.8 and 17.2 MPa) produced little difference in the bond quality and phases observed in the joint region, as previously observed for niobium and titanium diffusion bonds. The use of thicker molybdenum foil (25.4 μm) resulted in a significantly higher density of cracks in the bond region. As observed for titanium diffusion bonding, the use of a thinner foil generally improves the quality of the bond region. The phases in the bond region and bond quality were similar for diffusion bonding either hot-pressed SiC (α-SiC) or CVD SiC (β-SiC) with molybdenum foil.

Microprobe examination of the SiC/molybdenum-foil/SiC joint in Figure 4 shows that the bond region consists of two separate layers: (1) layer of molybdenum-silicide adjacent to the SiC interface that is either Mo_5Si_3 + carbon, Mo_5Si_3C or a mixture of these phases, and (2) a middle layer of molybdenum carbide (Mo_2C). Since carbon cannot be accurately quantified using EDS or WDS, it is difficult to determine if the outer layers are either Mo_5Si_3 + carbon, or Mo_5Si_3C, but carbon is clearly detected in these layers. The phases identified in the bond region of the SiC/molybdenum-foil/SiC joint in Figure 4 are the same as identified in previous work [6-8]. As observed for the niobium and titanium diffusion bonds, molybdenum diffusion bonding of CVD SiC (β-SiC) produces the same bond microstructure as observed for bonding with α-SiC base material. Solid-state diffusive reaction with SiC results in full conversion of the molybdenum foil into Mo_2C and Mo_5Si_3 + carbon or Mo_5Si_3C phases that are fairly brittle with a measurable volume change in Figure 4 ($20\mu m/12.5\mu m = 1.6$). However, the close CTE match for Mo_2C, which is a high fraction of the joint region, with SiC could result in less residual stresses, less defects, and less cracking in the bond region. The closer match in CTE and low volume change produced by diffusive conversion of the metal foil into carbide and silicide phases produces a higher quality joint with molybdenum diffusion bonding.

D. SiC/W/SiC Bond

A strong bond was produced for the SiC/tungsten-foil/SiC sandwich using Hexoloy™ SA SiC with 17.2 MPa applied pressure at 1500°C/10h (Table 1). A high density of cracks were observed in metallographic inspection of the bond joint region in Figure 5a. Although some of these defects may be artifacts of sample preparation, the high density of these defects indicates that the bond quality was not better than the molybdenum diffusion bonds.

EMP and SAM analysis in Figure 5 indicates that the 1 mil thick tungsten foil was fully converted into carbide and silicide phases with the following layered structure: (1) thin layer at the SiC interface containing tungsten and carbon in the levels consistent with the WC phase, and (2) a two-phase inner layer consisting of one phase containing primarily tungsten + carbon (W_2C) and a second phase containing primarily tungsten and silicon at the levels consistent with W_5Si_3. SAM analysis with depth profiling, which consists of spot analysis of the phases followed by repeated argon sputtering to clean the surface, was used to clearly identify the phases in the SiC/tungsten-foil/SiC bond region. A W_5Si_3 standard was used to confirm the

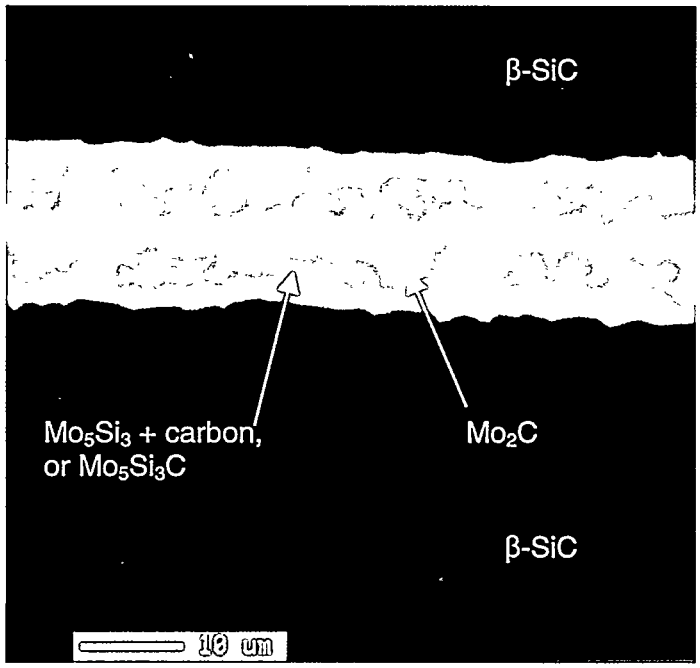

Figure 4. EMP analysis of the bond region microstructure of a SiC/molybdenum-foil/SiC bond produced under the parameters in Run #8 in Table 1.

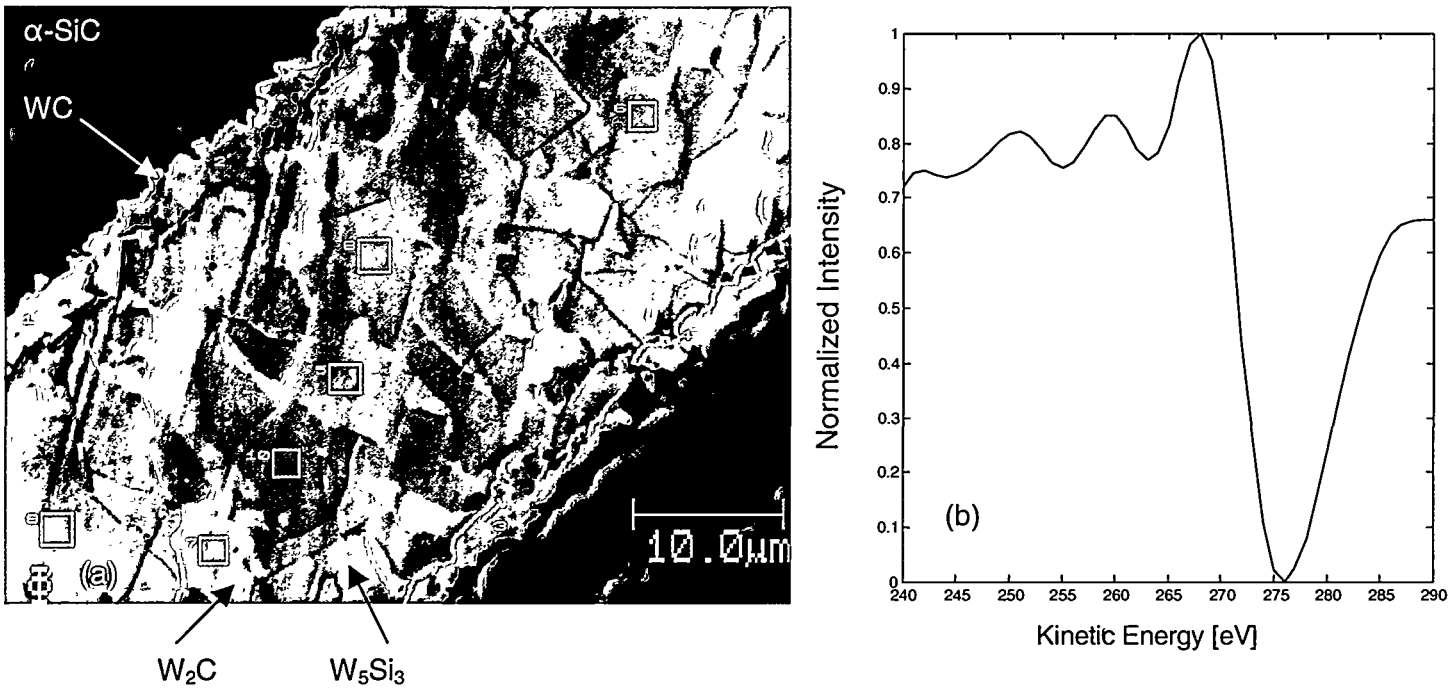

Auger chemical analysis determined by depth profiling from above [Compositions in Atomic%]

Area(s)	Number of Data Points	C	O	Si	W
1-4	35	49.1 ± 1.7	.3 ± .5	2.4 ± 2.7	48.3 ± 1.7
5-7	28	32.2 ± 1.4	.2 ± .2	5.2 ± 3.6	62.4 ± 3.1
8-10	30	1.9 ± .5	.2 ± .3	38.5 ± .8	59.5 ± .7

Figure 5. SAM analysis of the SiC/tungsten-foil/SiC bond region (Run #14 in Table 1): (a) micrograph of the SiC/tungsten-foil/SiC bond region showing the phases with a table for the phases identified, and (b) Auger spectra from a tungsten-carbide region showing the two peaks on the low energy side of the main carbon peak that signify a refractory metal carbide.

identity of the W_5Si_3 phase in the bond region. The carbon peak for both the WC and W_2C phases exhibit features that are consistent with refractory metal carbides, which is two small peaks at the lower energy side of the main carbon peak in Figure 5b. Previous evaluations of interdiffusion between tungsten foil and SiC were not found for comparison. Based on the microstructure examination of the SiC/tungsten-foil/SiC bond region, tungsten reacts with SiC by the diffusion path in Figure 6: SiC → WC → W_5Si_3 → W_2C → W.

Although the CTE for WC and SiC are similar (Figure 2), WC comprises a fairly small fraction of the bond region. The CTE for W_5Si_3 is significantly different than SiC [13] to provide the high density of cracks in the bond region. The volume increase resulting from the formation of the bond joint is not large (35μm/25μm = 1.4), which indicates that CTE differences likely produce the defects in the SiC/tungsten-foil/SiC bond region.

E. $^{11}B_4C$/Ti/$^{11}B_4C$ Bond

Strong bonding of $^{11}B_4C$ resulted from using a 5.1 μm thick titanium foil with 18.6 MPa pressure at 1500°C/10h, see Table 1. SAM and EMP analysis of the $^{11}B_4C$/titanium-foil/$^{11}B_4C$ bond region indicates that the microstructure consists of three layers, see Figure 7. The thin, recessed layer at the $^{11}B_4C$ interface contains a high amount of carbon with low levels of titanium and boron. This layer is likely carbon that is fairly soft, and may contain some polishing debris from metallographic preparation. The inner layer is a matrix of TiB_2 with fine precipitates. The central portion of the reaction zone contains a lower boron content and discrete regions that are high in carbon and contain titanium, which is consistent with TiB + TiC phases. Previous interdiffusion experiments between bulk titanium and B_4C at 750°C to 1000°C have indicated that a dual-layer reaction TiB/TiB_2 reaction zone containing TiC or $Ti(C,B)_x$ precipitates is formed [11]. The $^{11}B_4C$/titanium-foil/$^{11}B_4C$ bond region likely consists of carbon at the $^{11}B_4C$ interface, with TiB_2 and TiB + TiC in the central region. These results are

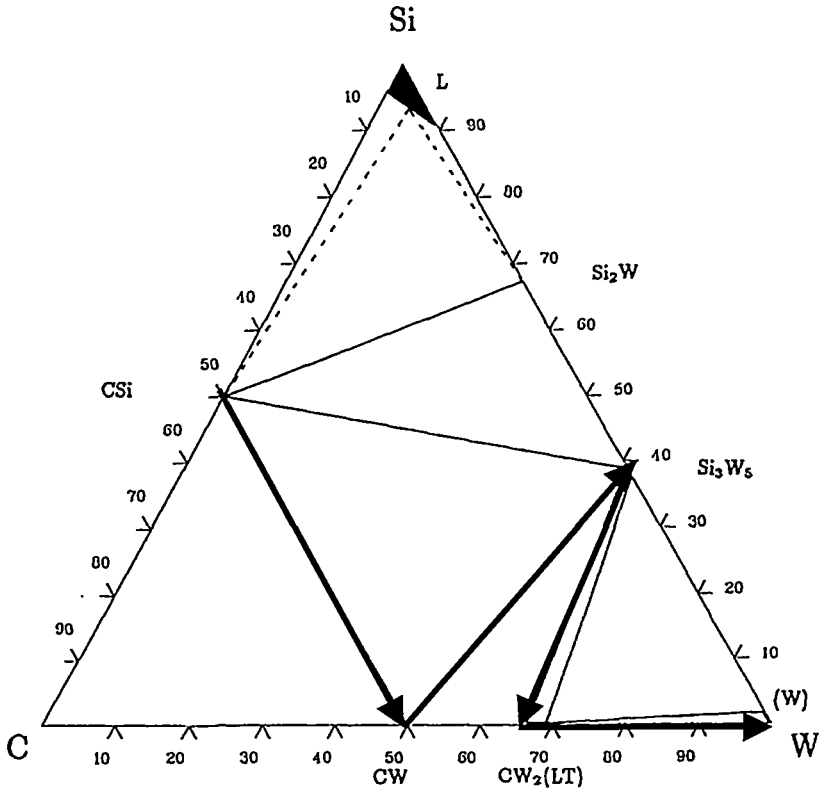

Figure 6. Reported isothermal section (1727°C) for the ternary diagram of the W-Si-C system [15]. The proposed diffusion path has been drawn: SiC → WC → W_5Si_3 → W_2C → W.

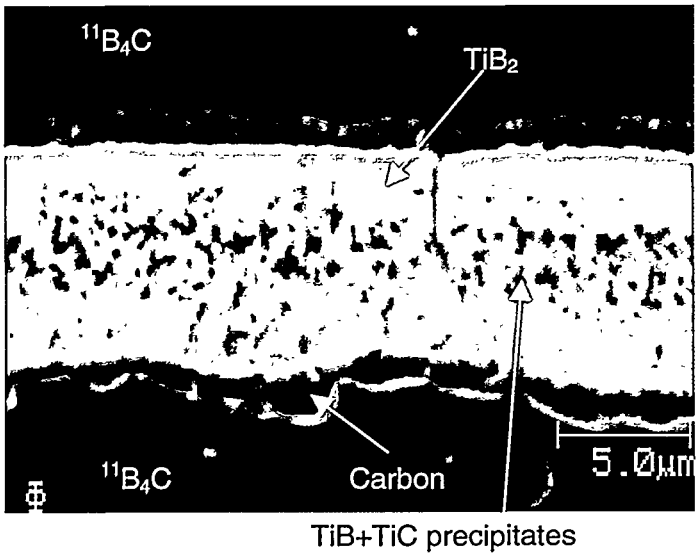

Figure 7. Section from the $^{11}B_4C$/titanium-foil/$^{11}B_4C$ joint region analyzed by SAM (Run #15 in Table 1).

somewhat consistent with previously reported phases for diffusion between bulk titanium and B_4C [12]. Assuming Ti(C,B) precipitates are not formed in the central region of the bond joint and based on these preliminary characterization results, the following diffusion path is proposed (Figure 8): Ti → TiB → TiC → TiB_2 → C → $^{11}B_4C$.

Previous work on titanium diffusion bonding of SiC indicated that the density of defects in the bond region was reduced when a thinner foil was used in the bonding process. Although thin titanium foil was used, the bond region of the $^{11}B_4C$/titanium-foil/$^{11}B_4C$ joint contained some cracks, but no regions of grain pullout, porosity, or interface delamination defects were resolved. The cracks could be artifacts of metallographic preparation, but the density of cracks indicates that the bond quality of the $^{11}B_4C$/titanium-foil/$^{11}B_4C$ joint was not the best.

F. $^{11}B_4C$/Mo/$^{11}B_4C$ Bond

A strong bond was produced with molybdenum foil using 18.6 MPa pressure at 1500°C for 10 hours, see Table 1. The use of EMP and SAM analysis indicates that the bond region of the $^{11}B_4C$/molybdenum-foil/$^{11}B_4C$ joint in Figure 9 consists of two layers that appear to contain second phase particles. The phase at the $^{11}B_4C$ interface is recessed and is rich in carbon with a small amount of molybdenum and boron. This layer is likely carbon with a small amount of molybdenum and boron that may be polishing debris. The middle layer consists of mainly two phases that are rich in molybdenum and boron: (1) phase with a high boron content, that is likely MoB, and (2) phase with a lower boron content that is likely Mo_2B. The middle region also contains fine carbon-rich precipitates, which could be either Mo_2C or Mo_2BC. Quantification of carbon and boron levels using EMP analysis was difficult. The use of SAM analysis was also complicated by an interference between an energy peak for molybdenum and boron.

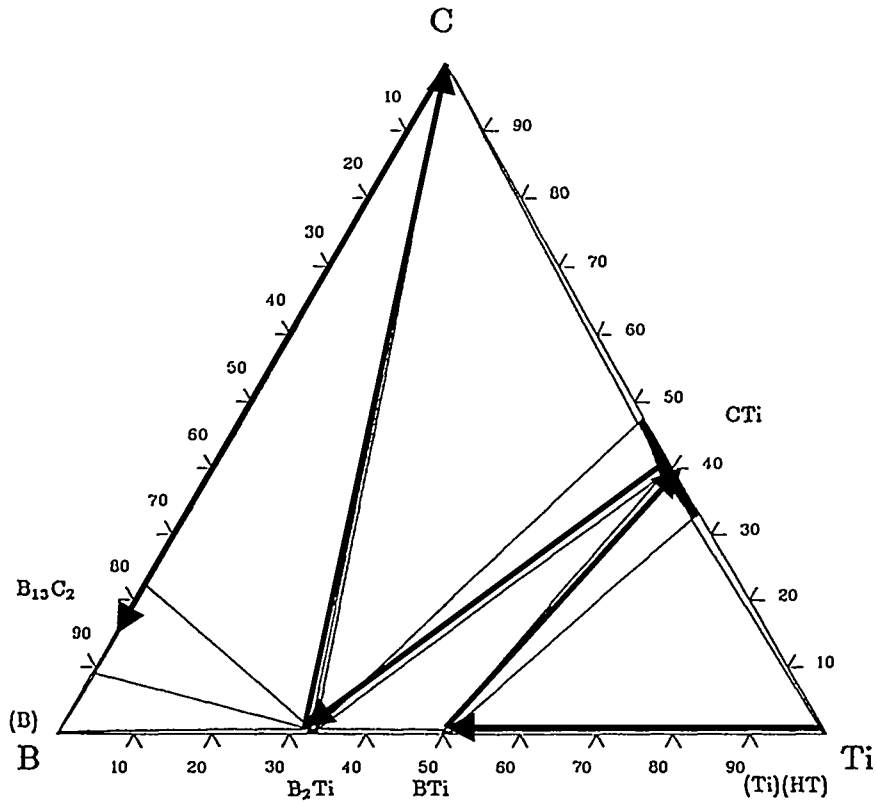

Figure 8. Reported ternary phase diagram for the isothermal section (1500°C) of the Ti-B-C system [16] with the proposed diffusion path: Ti → TiB → TiC → TiB_2 → C → $^{11}B_4C$.

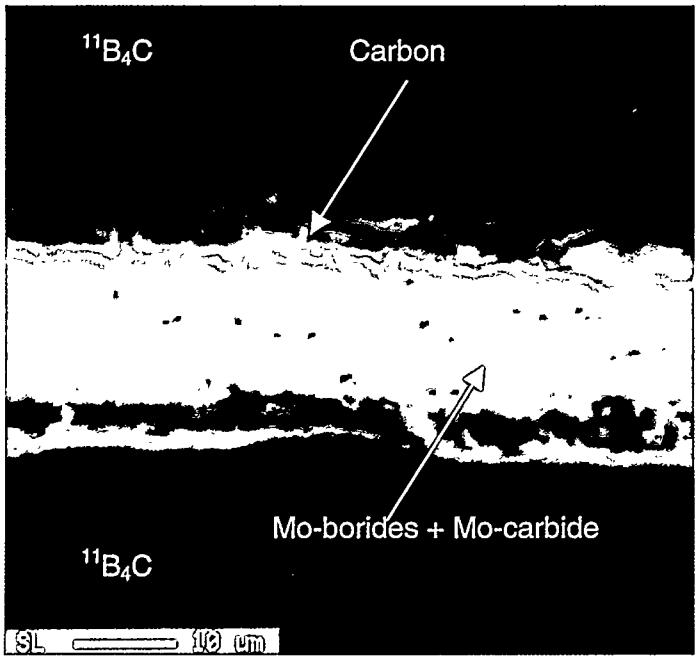

Figure 9. Section of the $^{11}B_4C$/molybdenum-foil/$^{11}B_4C$ bond region analyzed using SAM (Run #16 in Table 1).

Previous diffusion couple experiments between bulk molybdenum and B_4C at 1100°C to 1950°C have been reported to result in the formation of a two layer reaction zone of Mo_2B and MoB and each layer contained a dispersion of carbon precipitates [8]. Although the phase analysis of the bond region is not fully clear, the analysis of the $^{11}B_4C$/molybdenum-foil/$^{11}B_4C$ joint region is consistent with previous results [8]. Assuming the phases identified are correct, the interdiffusion between Mo and $^{11}B_4C$ probably occurs by one of the two possible diffusion paths: (1) Mo → Mo_2B → Mo_2C → MoB → C → $^{11}B_4C$, or (2) Mo → Mo_2B → Mo_2C → Mo_2BC → MoB → C → $^{11}B_4C$. However, more detailed phase analysis would be needed to clearly define the phases in the $^{11}B_4C$/Mo/$^{11}B_4C$ joint region.

The bond region of the $^{11}B_4C$/molybdenum-foil/$^{11}B_4C$ joint contains a lower density of defects such as cracks, regions of grain pullout, porosity, or interface delamination than the $^{11}B_4C$/titanium-foil/$^{11}B_4C$ joint. Based upon metallographic inspection of the bond regions, molybdenum foil diffusion bonding appears to be a good choice for bonding $^{11}B_4C$.

Summary

The use of niobium, titanium, molybdenum, and tungsten for metal foil diffusion bonding of SiC, and titanium and molybdenum for metal foil diffusion bonding of $^{11}B_4C$ was evaluated. The volume change resulting from the formation of the carbide and silicide compounds in the joint region (Table 1), and large CTE differences in the joint region between the carbide and silicide phases in the joint region and the SiC or the $^{11}B_4C$ base materials (Figure 2) results in the formation of cracks

in the bond region. The use of a higher bonding pressure had little influence on the quality of the bond region. The use of a thinner metal foil resulted in a significant decrease in the density of defects in the bond region for titanium and molybdenum diffusion bonding. The CTE differences between SiC and Mo_2C were generally lower than the phases in the bond regions produced with other foils, and a lower density of defects were observed in the bond region of joints produced by molybdenum foil diffusion bonding. This qualitative observation indicates that the bonds produced by molybdenum diffusion bonding are higher quality than bonds produced with niobium, titanium, or tungsten foils.

The majority of previous diffusion bonding work has involved the use of hot-pressed or sintered SiC (α-SiC structure), while most of this work involved the used of CVD SiC (β-SiC structure). The microstructure of the bond regions produced by niobium, titanium, or molybdenum diffusion bonding of β-SiC was similar to those produced with α-SiC base materials. Tungsten foil diffusion bonding, which has not been previously characterized, results in the formation of a WC layer at the SiC interface with an inner layer region of W_2C and W_5Si_3. This phase analysis is consistent with the following diffusion path for the SiC/tungsten-foil/SiC couple: SiC → WC → W_5Si_3 → W_2C → W.

Titanium foil diffusion bonding of $^{11}B_4C$ resulted in the formation of a bond region consisting of a layer of carbon with titanium and boron at the $^{11}B_4C$ interface with an inner layer consisting of TiB_2 and a central zone of TiB and TiC precipitates. The following diffusion path is proposed for the $^{11}B_4C$/titanium-foil/$^{11}B_4C$ couple: Ti → TiB → TiC → TiB_2 → C → $^{11}B_4C$. Molybdenum diffusion bonding of $^{11}B_4C$ resulted in the formation of a carbon layer containing molybdenum and boron at the $^{11}B_4C$ interface with an inner layer consisting of MoB and Mo_2B phases that contain Mo_2C or Mo_2BC precipitates. Due to the overlap of the molybdenum and boron peak, accurate phase analysis of the bond region of the molybdenum diffusion bond was not achieved. Based on metallographic inspections of the bonded $^{11}B_4C$ samples the molybdenum diffusion bond had a lower density of cracks and a higher bond quality.

Acknowledgement

This work was preformed under USDOE Contract DE-AC11-98PN38206. The helpful comments and contributions from J.L. Hollenbeck, W.L. Ohlinger, and F.W. Page are appreciated. The support of various Bettis personnel in completing this work is also appreciated (J.E. Cain, S.A. Vazquez, R.K. Ramaley, T.A. Dobrich, D.M. Gasparovic, A. Stinson, and D.L. Ward).

References

[1] A. Joshi, H.S. Hu, L. Jesion, J.J. Stephens, and J. Wadsworth, *Met. Trans.*, 21A, 2829-2837 (1990).

[2] M. Naka and J.C. Feng, *Trans. Mat. Res. Soc. Japan*, 16B, 1143-6 (1994).

[3] B. Gottselig, E. Gyarmati, A. Naoumidis, and H. Nickel, *J. European Ceramic Soc.*, 6, 153-160 (1990).

[4] S. Morozumi, M. Endo, M. Kikuchi, and K. Hamajima, *J. Mat. Sci.*, 20, 3976-3982 (1985).

[5] M. Naka, J.C. Feng, and J.C. Schuster, *Materials Trans. JIM*, 37, 394-398 (1996).

[6] K. Kurokawa and R. Nagasaki, *Proc. Int. Symp. & Exhibit on Sci. And Technol. Of Sintering*, Tokoyo, 1397-1402 (1987).

[7] A.E. Martinelli and R.A.L. Drew, *Mat. Sci. And Engg.*, A191, 239-247 (1995).

[8] S. Morozumi, M. Kikuchi, S. Sugai, and M. Hayashi, *J. Of Japan Inst. Of Metals*, 44, 1404-1412 (1980).

[9] H.O. Pierson, *Handbook of Refractory Carbides and Nitrides*, pp. 121-127, Noyes Publications, Westwood, New Jersey (1996).

[10] G. K. Kharchenko, N.A. Chaban, and V.F. Mazanko, *The Paton Welding Journal*, 46, 134-135 (1993).

[11] M.W. Chase, C.A. Davis, J.R. Downey, D.J. Frurip, R.A. McDonald, and A.N. Syverud, *JANAF Thermodynamical Tables, 3rd ed*, pp. 66-1108, APS, (1985).

[12] J. Thebault, R. Pailler, G. Bontemps-Moley, M. Bourdeau, and R. Naslain, *J. of the Less-Common Metals*, 47, 221-233 (1976).

[13] Y.S. Touloukian, R.K. Kirby, R.E. Taylor, and T.Y.R. Lee, *Thermophysical Properties of Matter: Vol. 13*, pp. 778-898, IFI-Plenum, New York (1977).

[14] M.W. Barsoum and T.E. Raghy, *J. Am. Ceram. Soc.*, 79, 1953-56 (1996).

[15] L. Brewer and O. Krikorian, *J. Electrochem. Soc.*, 103, 38-51 (1956).

[16] E. Rudy, *Ternary Phase Equilibria in Transition Metal-Boron-Carbon-Silicon Systems, Part V*, AFML-TR-65-2, p. 606 (1969).